

Microfluidic Multicolor Encoding of Microspheres with Nanoscopic Surface Complexity for Multiplex Immunoassays**

Shin-Hyun Kim,* Jae Won Shim, and Seung-Man Yang*

Suspension arrays have emerged as a promising tool for biological screening and multiplex immunoassays owing to several advantages over conventional 2D planar arrays, such as faster binding kinetics, large surface areas, increased statistical power, and low assay cost.^[1,2] Suspension arrays use identification tags on the microparticles rather than the spatial information employed in planar arrays. Two distinct approaches have been predominantly employed to write codes on particles in suspension arrays: spectrometric encoding and graphical encoding. In the first approach, the fluorescence spectra of polymeric microparticles are modulated by incorporating quantum dots or dye molecules with different emission wavelengths.^[1,3] Because photonic crystals exhibit bandgaps that depend on the lattice constant and refractive index contrast,^[4–6] the reflection spectra of photonic crystals can be also used as spectrometric codes. Graphical encoding methods, on the other hand, were developed to overcome the shortcomings of spectrometric encoding, which include insufficient distinct codes, spectral overlap between fluorescence from biomolecules and the code signal, and expensive decoding procedures.^[2,7] In graphical methods, microparticles are distinguished based on their shape or internal pattern, which can be modulated using lithographic techniques^[2,7–9] or direct writing,^[10] and are simply identified optically. Graphical encoding thus provides higher flexibility for target selection and faster and simpler decoding compared to spectrometric encoding. In many cases, however, the number of photomasks required is equal to the number of codes. Moreover, the expression of codes is complex and additional complicated procedures are needed for the surface functionalization of the polymeric microparticles.

Herein, we use a combination of the spectrometric and graphical encoding methods to develop a new and simple optofluidic approach to microsphere encoding based on a photocurable double-emulsion system. By using core droplets

with three distinct colors, namely red, green, and blue (RGB), we generated optically identifiable codes by controlling the numbers of the RGB core droplets encapsulated in the shell droplet. Because the RGB cores captured in the transparent shell can be identified without spectral analysis, the information can be decoded simply by counting the respective numbers of encapsulated RGB core droplets without the need for additional decoding equipment or devices. Furthermore, the abundance of achievable codes can be expressed using codes comprised of a few characters. On the other hand, the surface of each shell is decorated with an array of colloidal silica beads, which enables the creation of surface functional groups for immobilizing biomolecules.

To prepare double emulsion droplets in a precisely controlled manner, we employed a glass capillary device composed of three inner, one middle, and one outer capillary (Figure 1 a).^[11,12] Through the three inner capillaries, aqueous streams with RGB food coloring pigments were forced to flow while a photocurable silica suspension (ethoxylated trimethylolpropane triacrylate; ETPTA) and an aqueous surfactant solution were introduced in co-current mode through the middle and outer capillaries, respectively. In this way, the RGB core droplets were generated at the tips of the inner capillaries and subsequently encapsulated into a photocurable shell droplet at the tip of the middle capillary. Finally, the photocurable shells containing the aqueous RGB cores were solidified downstream under UV irradiation.

The number of RGB core droplets encapsulated in each particle can be controlled by varying the ratio of the generation frequencies of the cores and shells. Because the frequencies (f_{core} and f_{double}) can be controlled by the flow rates of the streams, the number N of encapsulated core droplets can be estimated by a simple mass balance:

$$N = \frac{f_{\text{core}}}{f_{\text{double}}} = \frac{Q_{\text{inner}}}{V_{\text{core}}} \frac{V_{\text{double}}}{(Q_{\text{inner}} + Q_{\text{middle}})} = \frac{V_{\text{double}}/V_{\text{core}}}{1 + Q_{\text{middle}}/Q_{\text{inner}}} \quad (1)$$

where Q_{inner} and Q_{middle} denote the volumetric flow rates of the inner and middle streams, respectively, and V_{core} and V_{double} are the volumes of the single core and single double emulsion droplets, respectively. Because V_{core} and V_{double} are predominantly determined by the flow rates of the middle and outer streams in dripping mode, respectively,^[13] the number of captured core droplets is determined by a combination of all inner, middle, and outer flow rates. Here, the above equation is applied independently for RGB cores with three sets of Q_{inner} , f_{core} , and N . As the simplest example, Figure 1 b shows the variation in the number of the captured cores as a function of $Q_{\text{middle}}/Q_{\text{inner}}$, together with images of the double-emulsion droplets of blue cores. In this plot, the solid curve corresponds

[*] Dr. S.-H. Kim, J. W. Shim, Prof. S.-M. Yang
National Creative Research Initiative Center for
Integrated Optofluidic Systems and
Department of Chemical and Biomolecular Engineering
KAIST, Daejeon, 305-701 (Korea)
Fax: (+82) 42-350-5962
E-mail: dmz@kaist.ac.kr
smyang@kaist.ac.kr
Homepage: http://msfl.kaist.ac.kr

[**] This work was supported by a grant from the Creative Research Initiative Program of the Ministry of Education, Science and Technology for "Complementary Hybridization of Optical and Fluidic Devices for Integrated Optofluidic Systems".

Supporting information for this article is available on the WWW under <http://dx.doi.org/10.1002/anie.201004869>.

to the case of $V_{\text{double}}/V_{\text{core}} = 101$. The deviation between the experimental points and the simple mass balance curve is caused by a small increase in V_{core} with increasing Q_{inner} . Movie S1 in the Supporting Information shows the generation of double-emulsion droplets containing a constant number of the core droplets. Furthermore, the generation of blue and green core droplets with relative frequencies of 1:1, 2:1, and 3:1 is displayed in Movie S2, and the resulting microspheres are shown in Figure S1 in the Supporting Information. Figure S2 shows droplet flows in downstream where the shell drops contain controlled numbers of RGB core droplets. Figure 1c shows representative examples of encoded microspheres with various numbers and colors of core droplets. Every code can be expressed simply with three characters and three numbers as “RXGYBZ” in which X, Y, and Z are the numbers of the RGB core droplets. For instance, the microspheres in the bottom image of the first column in Figure 1c

can be expressed as “B5”. In the same manner, the microspheres in the bottom images of the third and fifth columns can be expressed as “R5B5” and “R5G2B2”, respectively. Movie S3 shows a flow of “R1B2” droplets in the expansion channel and downstream, resulting in the microspheres in the top image of the fourth column in Figure 1c.

The number of possible codes (N_{code}) can be expressed with a simple combination calculus with repetition as follows:

$$N_{\text{code}} = \sum_{i=0}^N n H_i = \sum_{i=0}^N \sum_{n+i-1}^N C_i = \sum_{i=0}^N \frac{(n+i-1)!}{i!(n-1)!} \quad (2)$$

where N is the number of the controllable core droplets in a single shell and n is the number of colors of the core droplets. Therefore, a total of $N_{\text{code}} = 816$ different codes can be generated with 15 controllable core droplets of three different colors (that is, $N = 15$ and $n = 3$). For $N = 20$ and $n = 3$, the number of codes is almost doubled ($N_{\text{code}} = 1771$) and for $N = 20$ and $n = 5$, N_{code} increases to 53 130.

During and after the formation of the double emulsion droplets, the silica particles dispersed in the middle stream migrated spontaneously towards and anchored at the two interface types of the double emulsion droplets; that is, the interface between the core and the shell, and the interface between the shell and the continuous phase. The silica particles anchor at the free interfaces to reduce the total interfacial energy of the system. The energy reduction is sufficient such that particles are not dislodged from the interface by thermal motions.^[14,15] Therefore, the silica particle arrays at the inner interfaces stabilize the core droplets, thus preventing coalescence. On the other hand, the silica particles exposed to the continuous aqueous phase have surface silanol groups (SiOH), which through simple chemistry with a silane coupling agent can bind desired functional groups for immobilization of biomolecules (Figure 2a).

Figure 2b–d show SEM images of a microsphere with a hexagonal array of silica particles on its surface. The Moiré fringe evident in

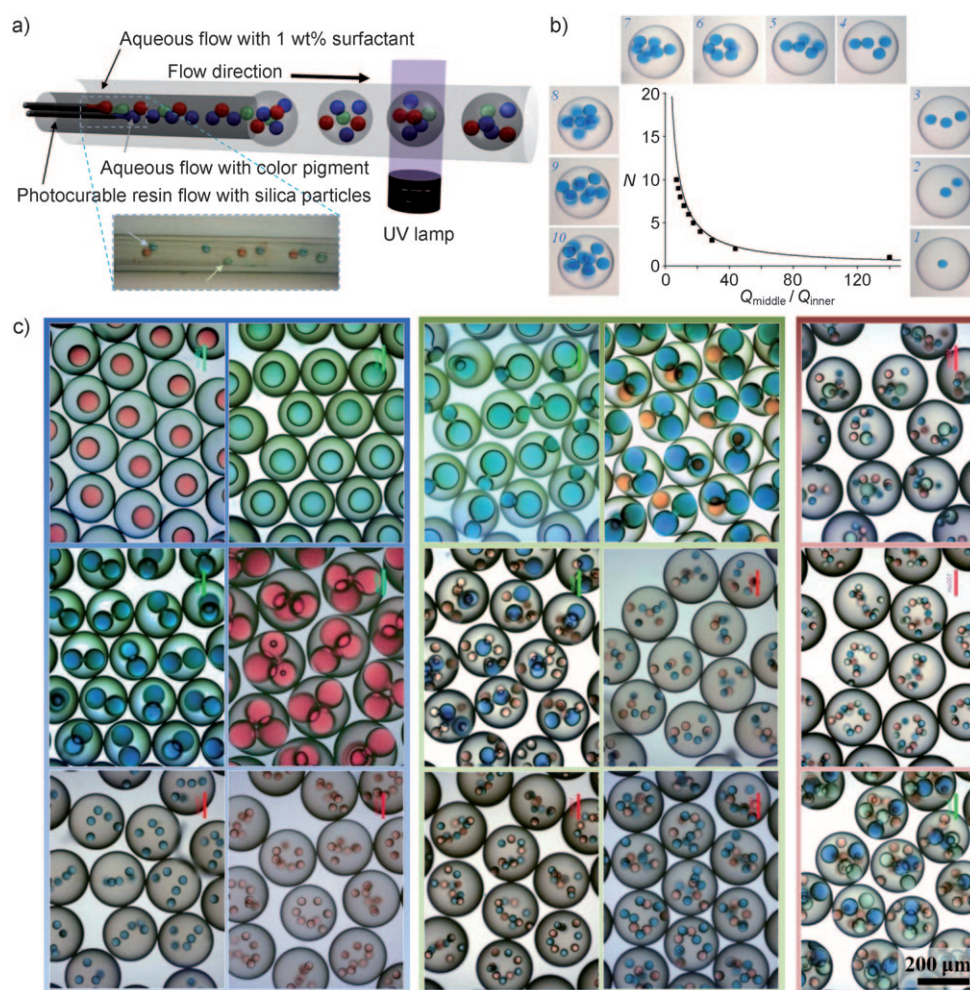


Figure 1. a) The microcapillary device equipped with a UV exposure unit for preparation of photocurable double emulsion droplets containing core droplets of three different colors. The inset shows an optical microscope image of the capillary device, where the tips for green and blue core droplets are included within the field of view (denoted with arrows). b) Control of the number of core droplets with relative volumetric flow rates of the middle to inner streams. Images of double emulsion droplets containing one to ten core droplets are shown. c) Examples of encoded microspheres. First two columns, second two columns, and last column show the microspheres encoded with core droplets of one color, two colors, and three colors, respectively.

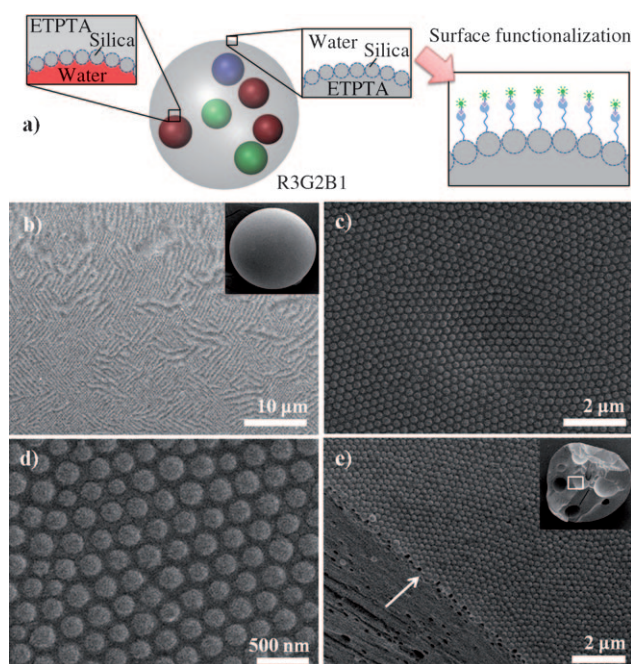


Figure 2. a) An encoded microsphere with silica particle arrays at the inner and outer surfaces. The silica particle arrays at the outer surface provide binding sites for biomolecules on the microsphere. b–d) SEM images of microsphere surfaces taken at different magnifications. In the images, Moiré fringes (b), a hexagonal array of silica particles (c), and partial exposure of silica particles to the surrounding medium (d) can be identified. The inset of (b) shows the spherical shape of the microspheres. e) SEM image of the inner surface of a broken microsphere (denoted as a white box in the inset). The arrow denotes the boundary between the polymeric matrix and the wall of the core droplet.

Figure 2b provides clear evidence of a highly ordered surface architecture over a large area. Figure 2c and d confirm the hexagonal array of silica particles and partial exposure of the silica particles to the surrounding medium, respectively. The SEM image in Figure 2e shows the inner surface of a broken microsphere with a hexagonal array of silica particles, which were originally anchored at the core droplet surface. A point that is worth stressing is that suspensions of the double emulsion droplets, as well as those of the microspheres formed after photopolymerization, are transparent. Unlike opaque common colloidal systems due to Mie scattering, the silica particles dispersed in the ETPTA shell droplet do not interrupt the identification of the colors of the core droplets. In the present systems, scattering is negligible owing to the small refractive index contrast between silica ($n_{\text{silica}} \approx 1.45$) and ETPTA ($n_{\text{ETPTA}} \approx 1.4689$).

We demonstrate multiplex immunoassays using three differently encoded microspheres, R7, R5B2, and R5G2B2, onto which we bound rabbit, human, and goat immunoglobulin G (IgG) protein molecules, respectively (Figure 3a–c). Briefly, the surfaces of the exposed silica particles on all microparticles were changed from silanol groups to amine and subsequently aldehyde groups. Then, the R7, R5B2, and R5G2B2 microspheres were treated with rabbit, human, and goat IgG, respectively.^[6b] After immobilization of the IgG

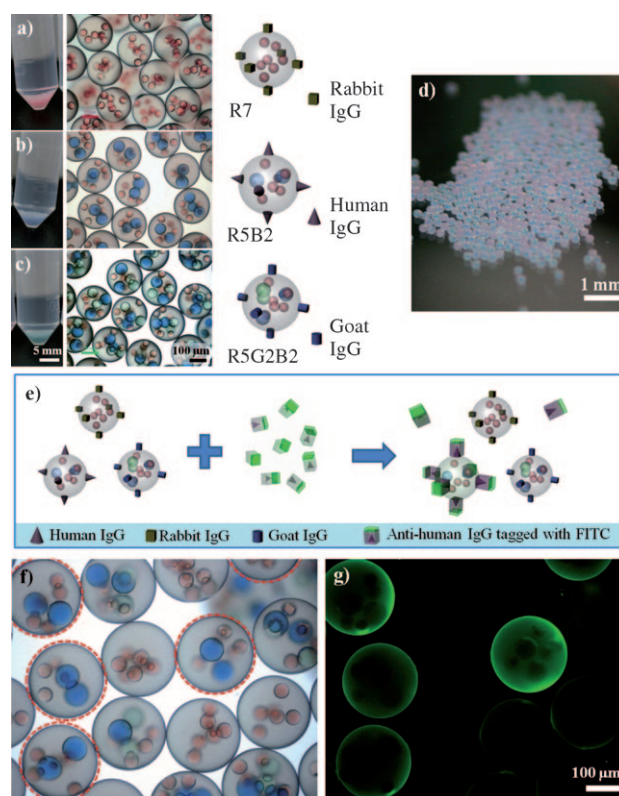


Figure 3. a) R7 microspheres treated with rabbit IgG: image in a tube, optical microscope image, and illustration of a microsphere treated with protein molecules. b, c) Similar sets of images for R5B2 with human IgG (b) and R5G2B2 with goat IgG (c). d) An image of a mixture of microspheres shown in (a–c). e) Illustration of an immunoassay. Anti-human IgG tagged with FITC will anchor only on the surfaces of the R5B2 microspheres. f, g) Optical (f) and fluorescence (g) microscope images of microsphere mixture after treatment with anti-human IgG taken at the same position. Only R5B2 microspheres, denoted as red-dotted circles in (f), show substantial fluorescence in (g).

molecules, the microspheres were treated with bovine serum albumin (BSA) to block any empty sites, thus preventing undesired adsorption. Into the mixture of three different microspheres (Figure 3d), we introduced anti-human IgG tagged with fluorescein isothiocyanate (FITC; Figure 3e). Among the three types of microsphere, strong fluorescence was observed only from R5B2, as can be seen in the optical and fluorescence microscope images in Figure 3f and g, respectively. This example demonstrates the potential utility of microspheres encoded with color cores in biological analysis. On the other hand, to inspect the sensitivity of microspheres, we treated human IgG-tagged microspheres with FITC-labeled anti-human IgG at various concentrations, as shown in Figure S3 in Supporting Information. By comparing the fluorescence from these particles with the weak fluorescence from untreated microspheres, we could detect anti-human IgG when the concentration was as low as 6.4 ng mL^{-1} .

In conclusion, we have developed a new and simple method for fabricating transparent microspheres and in situ multicolor encoding that combines the spectrometric and

graphical coding approaches. In the technique, a microfluidic device produced and manipulated double emulsion droplets of equal size with unprecedented controllability. The shell phase of the double emulsion droplets was then solidified by photopolymerization to produce transparent microspheres encoded with specific numbers of the core droplets with different colors, which can be identified optically. Importantly, we demonstrate multiplex immunoassay by employing the silica particle arrays on surfaces of the microspheres as efficient binding sites for immobilizing target biomolecules, by subtle surface chemistry. We believe that our microfluidic approach for microsphere encoding is useful in the field of microencapsulation and also various chemical and biological analyses.

Experimental Section

Preparation of the suspensions: Silica particles of diameter 230 nm were prepared by sol-gel chemistry using the Stöber method. An ethanolic suspension of the silica particles was mixed with an ETPTA resin (Aldrich) containing 1 wt % photoinitiator (Irgacure2100, Ciba Specialty Chemicals); after complete mixing, the ethanol was selectively evaporated for 12 h at 70°C. The quantities of silica particles and ETPTA were chosen such that the weight fraction of silica particles in ETPTA in the ethanol-free base was 10 % (w/w). The transparent silica-in-ETPTA suspension was sonicated for 30 min prior to use for droplet generation.

Preparation of encoded microspheres: To generate monodisperse double emulsion droplets, we employed a microfluidic device comprised of three inner, one middle, and one outer glass capillary (see Supporting Information for details of device fabrication). Through the three inner, one middle, and one outer capillaries, we introduced three aqueous solutions containing red, green, and blue food-coloring pigments, the silica-in-ETPTA suspension, and an aqueous solution of 1 wt % ethylene oxide-propylene oxide-ethylene oxide tri-block copolymer (Pluronic F108; BASF), respectively. The typical volumetric flow rates of the three inner, one middle, and one outer streams were 0.1, 2, and 300 $\mu\text{L min}^{-1}$, and were controlled independently by five syringe pumps (model 781200; KD Scientific). Core and shell droplets were generated at constant frequencies in dripping mode and double emulsion droplets were photopolymerized in the downstream region of the flow by passing through a UV irradiation zone. The prepared microspheres were collected in a glass Petri dish and washed several times to remove residual surfactant molecules.

Demonstration of multiplex immunoassays: To activate the silanol groups on the surfaces of the silica particles embedded in the microspheres, we treated the microspheres by immersion in 0.1M NaOH solution for 10 min. Subsequently, the microspheres were dispersed in 5 v/v % aqueous solution of 3-(aminopropyl)trimethox-

ysilane (APTMS) and reacted for 4 h under gentle shaking. The microspheres were then washed with phosphate buffer (PB; pH 5.7, 0.05 M) and dispersed and reacted in 2.5 v/v % glutaric dialdehyde in PB solution for 4 h. Next, the microspheres were washed with phosphate buffered saline (PBS; pH 7.4, 0.05 M) and reacted with 0.5 mg mL^{-1} rabbit, human, or goat IgG in PBS at 4°C for 12 h. After washing with PBS, the microspheres were treated with 1 % BSA in PBS at room temperature for 2 h and washed with PBS again. Finally, 20 $\mu\text{g mL}^{-1}$ anti-human IgG in PBS was added to the microsphere mixture and the system was maintained at 31 °C for 3 h. The resulting microspheres were washed with PBST (0.05 % Tween-20 in PBS solution) and water and observed using optical and fluorescence microscopy.

Received: August 5, 2010

Published online: December 22, 2010

Keywords: double emulsions · encoding · immunoassays · microfluidics · Pickering emulsions

- [1] M. Han, X. Gao, J. Z. Su, S. Nie, *Nat. Biotechnol.* **2001**, *19*, 631.
- [2] D. C. Pregibon, M. Toner, P. S. Doyle, *Science* **2007**, *315*, 1393.
- [3] B. J. Battersby, D. Bryant, W. Meutermaans, D. Matthews, M. L. Smythe, M. Trau, *J. Am. Chem. Soc.* **2000**, *122*, 2138.
- [4] F. Cunin, T. A. Schmedake, J. R. Link, Y. Y. Li, J. Koh, S. N. Bhatia, M. J. Sailor, *Nat. Mater.* **2002**, *1*, 39.
- [5] S. O. Meade, M. Y. Chen, M. J. Sailor, G. M. Miskelly, *Anal. Chem.* **2009**, *81*, 2618.
- [6] a) X. Zhao, Y. Cao, F. Ito, H.-H. Chen, K. Nagai, Y.-H. Zhao, Z.-Z. Gu, *Angew. Chem.* **2006**, *118*, 6989; *Angew. Chem. Int. Ed.* **2006**, *45*, 6835; b) Y. Zhao, X. Zhao, C. Sun, J. Li, R. Zhu, Z. Gu, *Anal. Chem.* **2008**, *80*, 1598.
- [7] Z. Zhi, Y. Morita, Q. Hasan, E. Tamiya, *Anal. Chem.* **2003**, *75*, 4125.
- [8] S. E. Chung, W. Park, H. Park, K. Yu, N. Park, S. Kwon, *Appl. Phys. Lett.* **2007**, *91*, 041106.
- [9] H.-Y. Chen, J.-M. Rouillard, E. Gulari, J. Lahann, *Proc. Natl. Acad. Sci. USA* **2007**, *104*, 11173.
- [10] K. Braeckmans, S. C. de Smedt, C. Roelant, M. Leblans, R. Pauwels, J. Demeester, *Nat. Mater.* **2003**, *2*, 169.
- [11] A. S. Utada, E. Lorenceau, D. R. Link, P. D. Kaplan, H. A. Stone, D. A. Weitz, *Science* **2005**, *308*, 537.
- [12] S.-H. Kim, S.-J. Jeon, S.-M. Yang, *J. Am. Chem. Soc.* **2008**, *130*, 6040.
- [13] A. S. Utada, A. Fernandez-Nieves, H. A. Stone, D. A. Weitz, *Phys. Rev. Lett.* **2007**, *99*, 094502.
- [14] B. P. Binks, S. O. Lumsdon, *Langmuir* **2000**, *16*, 8622.
- [15] a) A. B. Subramaniam, M. Abkarian, H. A. Stone, *Nat. Mater.* **2005**, *4*, 553; b) S.-H. Kim, S. Y. Lee, S.-M. Yang, *Angew. Chem.* **2010**, *122*, 2589; *Angew. Chem. Int. Ed.* **2010**, *49*, 2535.